Published OnlineFirst July 24, 2013; DOI: 10.1158/1535-7163.MCT-12-0962

Molecular Cancer Therapeutics

Catalase Abrogates β-Lapachone–Induced PARP1 Hyperactivation–Directed Programmed Necrosis in NQO1-Positive Breast Cancers

Erik A. Bey, Kathryn E. Reinicke, Melissa C. Srougi, et al.

Mol Cancer Ther 2013;12:2110-2120. Published OnlineFirst July 24, 2013.

Cancer Therapeutics Insights

Molecular Cancer Therapeutics

Catalase Abrogates β-Lapachone–Induced PARP1 Hyperactivation–Directed Programmed Necrosis in NQO1-Positive Breast Cancers

Erik A. Bey[1], Kathryn E. Reinicke[2], Melissa C. Srougi[3], Marie Varnes[2], Vernon E. Anderson[2], John J. Pink[4], Long Shan Li[5], Malina Patel[5], Lifen Cao[5], Zachary Moore[5], Amy Rommel[5], Michael Boatman[1], Cheryl Lewis[6], David M. Euhus[6], William G. Bornmann[7], Donald J. Buchsbaum[8], Douglas R. Spitz[9], Jinming Gao[5], and David A. Boothman[5]

Abstract

Improving patient outcome by personalized therapy involves a thorough understanding of an agent's mechanism of action. β-Lapachone (clinical forms, Arq501/Arq761) has been developed to exploit dramatic cancer-specific elevations in the phase II detoxifying enzyme NAD(P)H:quinone oxidoreductase (NQO1). NQO1 is dramatically elevated in solid cancers, including primary and metastatic [e.g., triple-negative (ER−, PR−, Her2/Neu−)] breast cancers. To define cellular factors that influence the efficacy of β-lapachone using knowledge of its mechanism of action, we confirmed that NQO1 was required for lethality and mediated a futile redox cycle where ∼120 moles of superoxide were formed per mole of β-lapachone in 2 minutes. β-Lapachone induced reactive oxygen species (ROS), stimulated DNA single-strand break-dependent poly(ADP-ribose) polymerase-1 (PARP1) hyperactivation, caused dramatic loss of essential nucleotides (NAD^+/ATP), and elicited programmed necrosis in breast cancer cells. Although PARP1 hyperactivation and NQO1 expression were major determinants of β-lapachone–induced lethality, alterations in catalase expression, including treatment with exogenous enzyme, caused marked cytoprotection. Thus, catalase is an important resistance factor and highlights H_2O_2 as an obligate ROS for cell death from this agent. Exogenous superoxide dismutase enhanced catalase-induced cytoprotection. β-Lapachone–induced cell death included apoptosis-inducing factor (AIF) translocation from mitochondria to nuclei, TUNEL+ staining, atypical PARP1 cleavage, and glyceraldehyde 3-phosphate dehydrogenase S-nitrosylation, which were abrogated by catalase. We predict that the ratio of NQO1:catalase activities in breast cancer versus associated normal tissue are likely to be the major determinants affecting the therapeutic window of β-lapachone and other NQO1 bioactivatable drugs. *Mol Cancer Ther; 12(10); 2110–20. ©2013 AACR.*

Authors' Affiliations: [1]Department of Basic Pharmaceutical Sciences, Mary Babb Randolph Cancer Center, West Virginia University, Morgantown, West Virginia; Departments of [2]Biochemistry, [3]Pharmacology, and [4]Oncology, Case Western Reserve University, Cleveland, Ohio; [5]Department of Pharmacology, Laboratory of Molecular Cell Stress Responses, Program in Cell Stress and Cancer Nanomedicine, Simmons Cancer Center; [6]Department of Surgery, UT Southwestern Medical Center at Dallas, Dallas; [7]Department of Experimental Therapeutics, MD Anderson Cancer Center, Houston, Texas; [8]Department of Radiation Oncology, University of Alabama-Birmingham, Birmingham, Alabama; and [9]Free Radical and Radiation Biology Program, Department of Radiation Oncology, Holden Comprehensive Cancer Center, University of Iowa, Iowa City, Iowa

Note: Supplementary data for this article are available at Molecular Cancer Therapeutics Online (http://mct.aacrjournals.org/).

Corresponding Authors: Erik A. Bey, West Virginia University, 1 Medical Center Drive, Box 9300, Room 1835, Morgantown, WV 26506. Phone: 214-645-6371; Fax: 214-645-6347; E-mail: ebey@hsc.wvu.edu; and David A. Boothman, University of Texas South Western Medical Center at Dallas, 6001 Forest Park Drive, ND2.210K, Mail stop 8807, Dallas, Texas 75390-8807; Email: David.Boothman@UTSouthwestern.edu

doi: 10.1158/1535-7163.MCT-12-0962

Introduction

Approximately 1 in 8 women will be diagnosed with breast cancer in their lifetimes in the United States (1). Most current therapeutic strategies designed to treat breast cancer, as with other cancers, attack proliferative differences between tumor and associated normal breast tissue. These approaches frequently result in minimal efficacy, undesirable normal tissue toxicity, and often result in selection of drug resistant, aggressive cancer cells undergoing epithelial-to-mesenchymal transition, with increased metastatic potential (2–5). Because caspase pathways are commonly abrogated or altered in breast or other cancers (6), strategies for treating cycling, as well as dormant cancer cells, that exploit caspase-independent cell death pathways (e.g., programmed necrosis) are desperately needed. Few drugs mechanistically act to induce poly(ADP-ribose) polymerase-1 (PARP1)-mediated programmed necrosis in a tumor-specific manner and at clinically relevant doses (7). Most

agents known to stimulate PARP1-mediated programmed necrosis (e.g., N-methyl, N′-nitro, N-nitrosoguanidine (>5 mmol/L MNNG), or hydrogen peroxide (>200 μmol/L H_2O_2; refs. 8–10) do so at supra-lethal, nonachievable doses clinically. In contrast, β-lapachone (β-lap; see Fig. 1 for structure) stimulates PARP1 hyperactivation and causes dramatic intracellular nucleotide loss, particularly in NAD^+ and ATP pools (10), at clinically achievable doses. PARP1 uses NAD^+ as a substrate to conduct poly(ADP-ribosylation) (PAR) posttranslational modification of proteins, including itself, where poly (ADP-ribosylated)-PARP1 (PAR-PARP1) is functionally inactive.

β-Lap is efficacious against solid tumors that have endogenously overexpressed NAD(P)H:quinone oxidoreductase I (NQO1), including >80% non–small cell lung and pancreatic, as well as >60% prostate and >70% breast cancers, where 5- to >100-fold increases in NQO1 activities above adjacent normal tissue were reported (11–13). β-Lap undergoes an NQO1-dependent futile redox cycle (Fig. 1A), where >60 moles of NAD(P)H are consumed per mole β-lap in 1 to 2 minutes (12, 14–18). This futile cycle results from the instability of its hydroquinone and semiquinone forms, presumably consuming oxygen and theoretically creating dramatically elevated levels of superoxide ($O_2^{\cdot -}$). Combined DNA damage and Ca^{2+} release from endoplasmic reticulum ($Ca^{2+}{}_{ER}$) stores culminates in PARP1 hyperactivation, NAD^+/ATP loss, DNA repair inhibition, and programmed necrosis by unknown protein effectors (12, 16–19). The majority of reported cellular affects in β-lap–treated cancer cells are actually the result of dramatic NAD^+/ATP losses (reviewed in ref. 20). Understanding the role(s) of reactive oxygen species

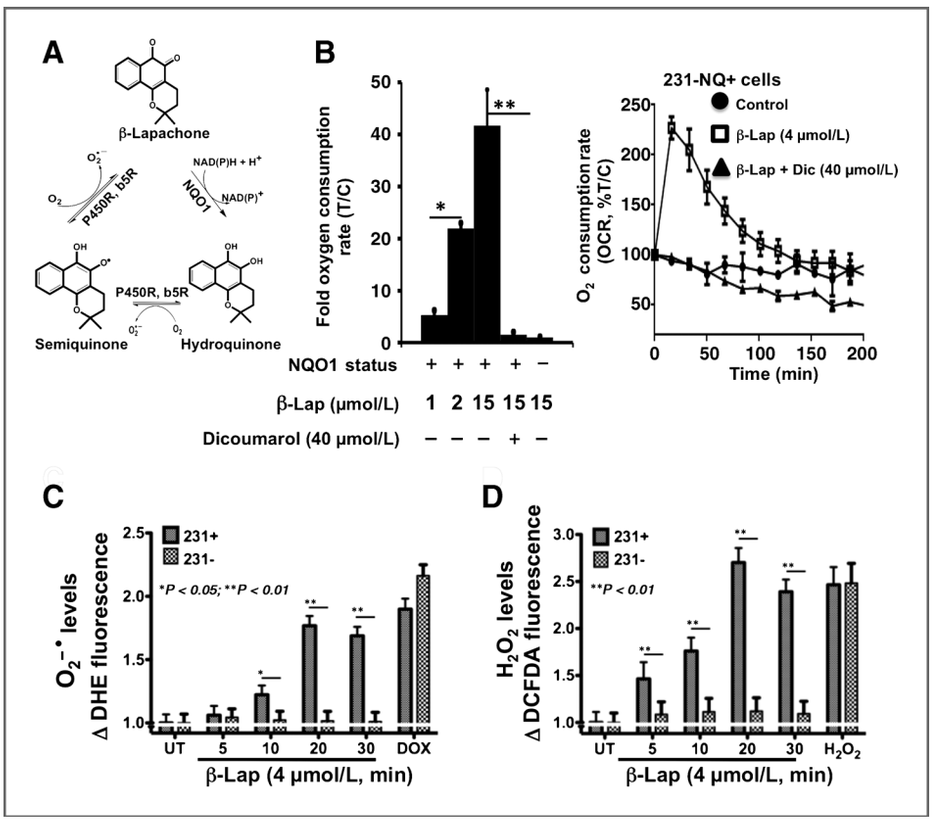

Figure 1. NQO1-dependent futile redox cycling of β-lap consumes O_2 and generates robust ROS. A, proposed futile redox cycle of β-lap in the presence of NQO1, where the hydroquinone form of β-lap is unstable. Through 2 one-electron oxidations, which presumably use O_2, the hydroquinone spontaneously reverts back to β-lap. This "bioactivatable redox cycle" of β-lap uses ≥60 moles NAD(P)H/mole β-lap in 2 minutes (15), consuming 2 moles O_2 per cycle, creating ~120 moles superoxide in 2 minutes. B (left), cell extracts from NQO1-expressing (231-NQ+) or NQO1-deficient (231-NQ−) MDA-MB-231 TNBC cells were placed in a closed system with 1, 2, or 15 μmol/L β-lap, ± dicoumarol (DIC), an NQO1 inhibitor, for 5 minutes. OCR was measured with an Ocean Optics O_2 sensor (left) as described in Materials and Methods. Each bar represents X-fold OCR means ± SE, of 2 independent experiments conducted in triplicate. *, $P \leq 0.05$ (1 vs. 2 μmol/L β-lap); **, $P \leq 0.007$ (15 μmol/L β-lap ± 40 μmol/L DIC). B (right), O_2 consumption rates and proton production rates were measured in mock-treated (control) or β-Lap 4 μmol/L exposed 231-NQ+ cells ± 40 μmol/L DIC using the Seahorse XF24 Analyzer and Assay Wizard software. Data represent means, percentage treated/control (T/C, %) ±SE from quadruplicate samples. C and D, β-Lap–treated 231-NQ+ and 231-NQ− cells were analyzed for ROS formation at indicated times. Cells were stained with DHE (for $O_2^{\cdot -}$) in C, or DCFDA (H_2O_2) in D, and micrographs quantified as described (17) and in Materials and Methods. DOX (5 μmol/L, 30 minutes), H_2O_2 (200 μmol/L, 30 minutes) were used as positive controls. Student *t* tests were conducted to determine significance between means of treatment conditions conducted in triplicate, repeated 3 individual times.

(ROS) and ROS-scavenging enzymes in deterring the efficacy of β-lap or deoxynyboquinone (DNQ), the only other NQO1 bioactivatable drug (7) against NQO1 overexpressed solid cancers remains unexplored.

Here, we report a potential mechanism of resistance to β-lap–induced cell death by catalase, potentiated by superoxide dismutase (SOD). PARP1 hyperactivation was the major determinant of downstream-programmed necrosis initiation when sublethal to lethal doses of β-lap were compared. Exposure of NQO1+ cells to sublethal β-lap doses (≤1 μmol/L) caused enhanced O_2 consumption, ROS formation and single-strand breaks (SSBs); however, DNA lesions were below an apparent "threshold damage level" required for PARP1 hyperactivation. In contrast, lethal β-lap doses (≥2 μmol/L) that killed ≥50% NQO1+ MDA-MB-231 triple-negative breast cancer cells (TNBC, Supplemental Table S1) stimulated PARP1 hyperactivation causing dramatic NAD^+/ATP losses. As a result, apoptosis inducing factor (AIF) activation and glyceraldehyde 3-phosphate dehydrogenase (GAPDH) modification were noted that corresponded to programmed necrosis. Catalase spared β-lap–treated cells from H_2O_2 (but not $O_2^{\cdot-}$) formation, PARP1 hyperactivation, AIF activation, atypical PARP1 and p53 proteolysis, blocked TUNEL+ staining, and enhanced clonogenic survival. The cytoprotective effects of catalase were enhanced by SOD co-addition, consistent with an obligate role of H_2O_2 in β-lap–induced lethality. Although inhibiting AIF expression slightly protected cells from β-lap–induced lethality, altering downstream protein effectors were much less effective than altering upstream processes, such as scavenging ROS or chelating $Ca^{2+}{}_{ER}$ at preventing lethality. The ratio of NQO1/catalase expression in tumor versus normal tissue may be a major determinant in the efficacy of antitumor regimen involving NQO1 bioactivatable drugs, such as β-lap.

Materials and Methods

Chemicals, reagents, and antibodies

β-Lap (3,4-dihydro-2,2-dimethyl-2*H*-naphtho[1,2-*b*]pyran-5,6-dione; Fig. 1) was synthesized by us, confirmed by NMR, dissolved in DMSO at 50 μmol/L, and concentrations verified by spectrophotometry (15). Menadione and doxorubicin (DOX) were obtained from Sigma-Aldrich and dissolved in DMSO or PBS (DOX), respectively. Dicoumarol (DIC; Sigma-Aldrich) was used as described (15). 5-(and-6)Chloromethyl-2,7-dichlorodihydrofluorescein diacetate (DCFDA, 5 μmol/L) and dihydroethidium (DHE, 5 μmol/L) used to assess ROS formation were purchased from Invitrogen and used as described previously (18, 19). *N*-Acetyl-L-cysteine (NAC; Sigma-Aldrich) was used at 5 mmol/L for 24-hour pretreatments and 2-hour cotreatments as described (21). Xanthine, nitroblue tetrazolium, diethylenetriaminepentaacetic acid, catalase, CuZnSOD, bovine serum albumin (BSA), bathocuproine disulfonic acid disodium salt hydrate, and xanthine oxidase (Sigma-Aldrich) were used as described (22). Staurosporine (STS) and the pan-caspase inhibitor, zVAD-FMK (Z-VAD), were obtained and used as described (refs. 12, 14–18; see structures, Supplemental Fig. S1). In transient AIF knockdown experiments, AIF (siAIF), NQO1 (si-NQ), and scrambled control vector (SCR) siRNAs were purchased from (Dharmacon).

Cell lines, cell culture, treatments, and survival

MDA-MB-231 TNBC cells lacking or expressing NQO1 and MCF-7:WS8 (MCF-7) cells were grown as described (15, 17). Additional breast cancer cell lines were purchased from ATTC, MAP-tested and were free of mycoplasma. Breast cancer cell lines were grown in RPMI 1640 media at 37°C in a humidified 10% CO_2-95% air atmosphere. Human mammary epithelial cells (HMEC 1585) were isolated from normal human mammary epithelial tissue of a patient without breast cancer and subjected to DNA finger printing. HMEC were grown in MEGM/DMEM-F12 complete media (Lonza and Mediatech) at 37°C in a humidified 5% CO_2-95% air atmosphere. Relative survival assays were conducted as described (15). Experiments were repeated at least 3 times, and data expressed as relative survival (treated/control × 100%) means ± SE. Results using this assay directly correlated with clonogenic assays (15). A multitarget model was used to describe the shape of relative survival curves, where the final slope (D_0) and quasi-threshold (D_q) doses were used to represent the size or width of the shoulder. Three parameters, n (extrapolation number), D_0, and D_q were related as: $\log_e n = D_q/D_0$. In experiments with catalase, bovine catalase (Sigma-Aldrich) was dissolved in 5 mmol/L Hepes buffer (pH 7.4) or PBS. Dissolved catalase was filter sterilized and added to drug media before exposure to drug treatment. O_2 consumption rates (OCR) were measured using an Ocean Optics, Inc. Foxy-18G-AF oxygen sensor and S9 supernatants (15). S9 extracts were added to a closed system in Tris-HCl buffer containing 10% BSA, pH 7.5, 0.5 mmol/L NADH, β-lap ± 40 μmol/L DIC (23). The OOISensors program (Ocean Optics, Inc.) was used to quantify fluorescence at 599.62 nm every 512 seconds, averaging every 4 readings. Data (means ± SE) were graphed as X-fold OCR from 3 independent experiments, each conducted in triplicate. In addition to Ocean Optics experiments, OCRs were confirmed in 231-NQ+ and 231-NQ− cells using a Seahorse XF24 extracellular flux analyzer (Seahorse Biosciences) as described previously (7). Briefly 25,000 231-NQ+ or 231-NQ− cells were seeded in Seahorse 24-well microplates. Before analysis, cells were left untreated (control) or treated with 4 μmol/L β-lap with or without DIC. OCR were measured as previously described (7). Data represent means, % treated/control (%T/C), ±SE from quadruplicate assessments.

ROS, NAD^+, and ATP measurements

Cellular oxidative stress was assessed by reduced/total glutathione, %GSSG content (17), and normalized to protein (24). Experiments were conducted 3 times and data

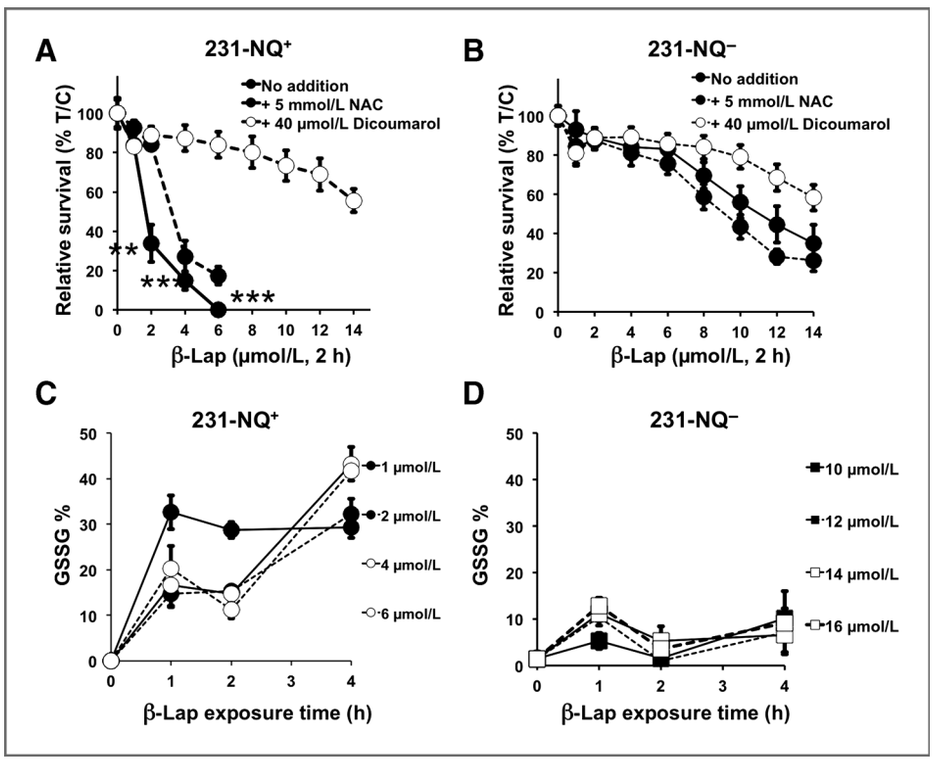

Figure 2. NQO1-dependent, β-lap–induced oxidative stress correlates with lethality. A and B, 231-NQ+ and 231-NQ− cells were exposed to β-lap (μmol/L, 2 hours) with or without 5 mmol/L NAC or 40 μmol/L dicoumarol and survival was determined (17). **, $P \leq 0.01$; ***, $P \leq 0.001$. C and D, 231-NQ+ and 231-NQ− cells were exposed to indicated β-lap doses for varying times and reduced glutathione levels (% GSSG) assessed (17). Student *t* tests were conducted and differences between means from 3 independent experiments were performed in sextuplet (A and B) or triplicate (C and D).

expressed as means ± SE. ROS formation was assessed microscopically in 231 NQ+ and NQ− cells stained with DCFDA or DHE. Quantitative data obtained from digital images of at least 100 cells were analyzed using NIH ImageJ software. Changes in intracellular NAD^+ levels were measured (17) and data expressed as $\%NAD^+$ (% treated/control) means ± SE for experiments conducted 3 times in triplicate.

Comet assays

DNA damage was assessed by alkaline comet assays, tail migration distance measured and analyzed using NIH ImageJ software (17). Comet tail lengths were measured in micrometers and mean lengths ± SE reported from 3 independent experiments conducted in triplicate.

Apoptosis

TUNEL assays were conducted (16) and data expressed as means ± SE from 3 separate experiments.

Western blotting and antibodies

Western blot analyses were conducted as described (15). α-PAR and α-γ-H_2AX were used as described (17). α-PARP1 (SC-8007, 1:2,000), α-AIF (SC-5586, 1:2,000), α-tubulin (1:10,000), and α-GAPDH (SC-25778 and 32233, 1:50,000) were from Santa Cruz. Additional α-GAPDH antibodies (CB-1001, 1:50,000) and (ab-9485, 1:50,000) were purchased from Calbiochem and from Abcam, respectively. Relative PAR levels were calculated by densitometric analyses using NIH ImageJ using PARP1 loading controls. Measurements were normalized to $t = 0$ levels. Western blots shown were representative of separate experiments conducted at least 3 times.

Statistics

All experiments were repeated at least twice in triplicate. Student *t* tests were conducted to compare conditions and data were reported as means ± SE.

Results

β-Lap-induced, NQO1-dependent O_2 consumption

NQO1-driven futile redox cycling of β-lap (Fig. 1A; ref. 15) predicted a robust OCR, with concomitant rapid and dramatic $O_2^{\cdot-}$ and H_2O_2 formation. Using MDA-MB-231 TNBC cells expressing (231-NQ+) or lacking (231-NQ−) NQO1, we directly measured OCR in a closed system with an Ocean Optics O_2 sensor (Fig. 1B, left). Appropriate controls using KCN and oligomycin, inhibitors of the electron transport chain, were conducted (Supplementary Fig. S2). NADH, β-lap, and NQO1 enzymatic activity were necessary components for robust futile redox cycling and elevated OCR, because DIC prevented dose-dependent, β-lap–induced OCR increases (~40-fold in 5 minutes after 15 μmol/L) in 231-NQ+ cells. Significant increases in OCR were noted in NQO1+ cells exposed to 2 μmol/L versus 1 μmol/L β-lap (Fig. 1B, left). In contrast, 231-NQ− cells showed no OCR increases after β-lap, up to 15 μmol/L (Fig. 1B, left). OCRs in 231-NQ+ cells exposed to 4 μmol/L β-lap were then confirmed

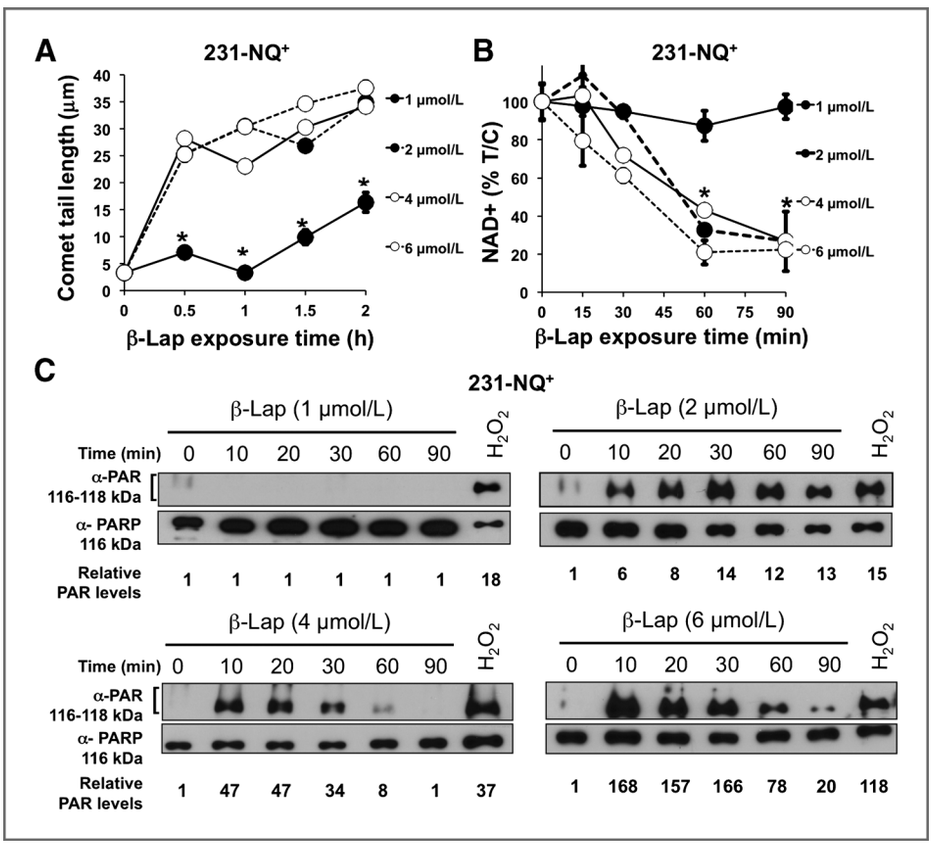

Figure 3. PARP1 hyperactivation is a determining factor in β-lap–induced programmed necrosis. A, 231-NQ+ cells were treated with various β-lap doses as indicated and total DNA damage was measured by alkaline comet assays. Comet tails, a measure of DNA damage, were quantified using ImageJ software (17) and means ± SE from 50 individual cells per group from 3 independent experiments were measured. *, $P \leq 0.01$ (to 6 μmol/L, β-lap). B, 231-NQ+ cells were treated with β-lap doses (1, 2, 4, or 6 μmol/L) for the indicated times. Changes in NAD^+ content were measured (18). C, 231-NQ+ cells were treated with various β-lap doses for the indicated times and PARP1 hyperactivation monitored by PAR-PARP1 formation. PAR-modified PARP-1 seen as 116 to 118 kDa bands and represents inactive PARP1. H_2O_2 (200 μmol/L, 60 minutes) was used as a positive control for PAR-PARP1 formation. Shown are representative Western blots of experiments conducted at least 3 times.

using the Seahorse monitoring systems as previously described (7). β-Lap (4 μmol/L) exposure caused an immediate burst in OCRs that were inhibited by DIC, and dissipated over the next 100 minutes (Fig. 1B, right). NQO1-dependent OCRs were accompanied by dramatic increases in $O_2^{\cdot -}$ (Fig. 1C) and H_2O_2 (Fig. 1D). The absence of significant ROS in NQO1- cells strongly suggested that within the 2 to 4 hours exposure of cells to β-lap (4 μmol/L), the drug was a relatively poor substrate for one-electron oxidoreductions, mediated by b5R and p450R oxidoreductases (ref. 17; Fig. 1A). Cells exposed to DOX (5 μmol/L, 30 minutes) or H_2O_2 (200 μmol/L, 30 minutes) resulted in statistically equivalent $O_2^{\cdot}$ or H_2O_2 levels, respectively, in 231-NQ− or 231-NQ+ cells (Fig. 1C and D), suggesting that scavenging enzymes/factors present were equivalent in these NQO1 isogenic cells.

Lethal β-lap doses cause threshold levels of DNA damage required for PARP1 hyperactivation

Survival responses of NQO1+ human cancer cells to increasing β-lap concentrations are rather sharp, where 1 to 1.8 μmol/L treatments for 2 to 4 hours were not lethal, but incremental increases to 2 to 3 μmol/L caused >90% cell death responses, indicated by strong TUNEL+ staining (15, 17, 21). We hypothesized that these sharp dose–responses were due not only to futile redox cycling of β-lap in NQO1+ cells expressing ~100 units of NQO1 (19), but that differences between sublethal and lethal doses of the drug were due to achieving a critical threshold level of DNA lesions (specifically base damage and SSBs) that ultimately hyperactivate PARP1. We characterized sublethal (1 μmol/L, 2 hours) and lethal (≥2 μmol/L, 2 hours) β-lap doses in 231-NQ+ cells (Fig. 2A), whereas 231-NQ− cells and normal primary human mammary epithelial cells remained nonresponsive at either dose (Fig. 2B, Supplementary Fig. S3). ROS generation over time (%GSSG formation) in 231-NQ+ cells exposed to lethal versus sublethal β-lap doses indicated no statistical differences ($P > 0.5$; Fig. 2C) between treatments; use of %GSSG as an indicator of ROS was apparently not as sensitive an endpoint to discriminate sublethal versus lethal doses of β-lap (Fig. 2C) compared to use of indicator dyes (Fig. 1C and D). Interestingly, the chemical ROS scavenger, NAC (given as pre- and cotreatments with β-lap), only partially protected cells against the lethal effects of 2, but not 3 μmol/L, β-lap (Fig. 2A). However, when NQO1 levels were partially inhibited by DIC, the efficacy of NAC was dramatically improved (Supplementary Fig. S4), suggesting that NQO1-dependent redox cycling of β-lap produced ROS that could easily swamp the ROS-scavenging effects of

NAC. In contrast, only minor levels of oxidative stress were noted in 231-NQ− cells at any β-lap dose tested using GSSG assays (Fig. 2D). These data suggested that although ROS scavengers were easily overwhelmed at low β-lap doses, factors such as NAC may play significant roles in protecting cells from sublethal or LD_{50} doses that might be used in combination therapies (14).

Alkaline comet assays were then used to assess the extent of total DNA lesions (base damage, SSBs, and double-strand breaks) created by various β-lap doses in 231-NQ+ versus 231-NQ− cells (Fig. 3A and B). Although a sublethal 1 μmol/L β-lap dose produced significant GSSG formation (Fig. 2C), this exposure caused significantly less DNA damage versus a lethal dose (2 μmol/L an ~LD_{70}; Fig. 3A). All lethal β-lap doses (2–6 μmol/L; Fig. 3A) caused similar saturating levels of DNA lesions, consistent with elevated and saturated oxidized GSSG levels (Fig. 2C). In contrast, β-lap treatment of 231-NQ− cells did not result in significant DNA lesions, consistent with the lack of OCR, ROS (H_2O_2) formation and lethality in NQO1− cells.

Exposure of 231-NQ+ cells to a nonlethal β-lap (1 μmol/L) dose did not result in measurable DNA lesions, loss of NAD^+ or PAR-PARP1 formation (Fig. 3A and C). In contrast, treatment of NQO1+ cells with cytotoxic β-lap doses (≥2 μmol/L) resulted in significant NAD^+ pool loss (Fig. 3B) and PAR-PARP1 formation (Fig. 3C), consistent with PARP1 hyperactivation (17), and steady-state accumulation of posttranslational PAR-modified and inactivated PARP1 (PAR; Fig. 3C). Peak PAR-PARP1 formation was noted 30 minutes after 2 μmol/L β-lap, whose time to peak levels decreased with increasing doses (Fig. 3C; compare 2–6 μmol/L β-lap exposures). Interestingly, loss of intracellular NAD^+ levels were similar with all lethal doses of β-lap, strongly suggesting saturated PARP1 hyperactivation at all doses (Fig. 3B).

Catalase detoxifies β-lap–induced H_2O_2 formation and is cytoprotective

Exogenous catalase (1,000 U) significantly lowered H_2O_2 levels in β-lap–exposed 231-NQ+ cells (Fig. 4A, left), whereas its addition had no affect on $O_2^{\cdot-}$ formation (not shown). Similarly, exogenous $CuZn^{2+}$-dependent superoxide dismutase (CuZnSOD, 3,000 U) decreased $O_2^{\cdot-}$ formation (Fig. 4A, right), whereas slightly increasing H_2O_2 levels (not shown). Forced overexpression of catalase in NQO1+ MCF-7 cells (Fig. 4B) using a CMV-driven expression vector (Open Biosystems) significantly spared NQO1+ MCF-7 cells from lethal β-lap doses (Fig. 4C), ranging from 2 to 4 μmol/L.

Similarly, exogenous catalase (≥500 U) significantly protected 231-NQ+ cells from β-lap lethality (Fig. 5A), whereas the survival of β-lap–treated 231-NQ− cells were not affected by the drug, with or without catalase coaddition (Fig. 5B). Exogenous coadministration of catalase with CuZnSOD significantly decreased the effective catalase dose required to prevent β-lap–induced lethality

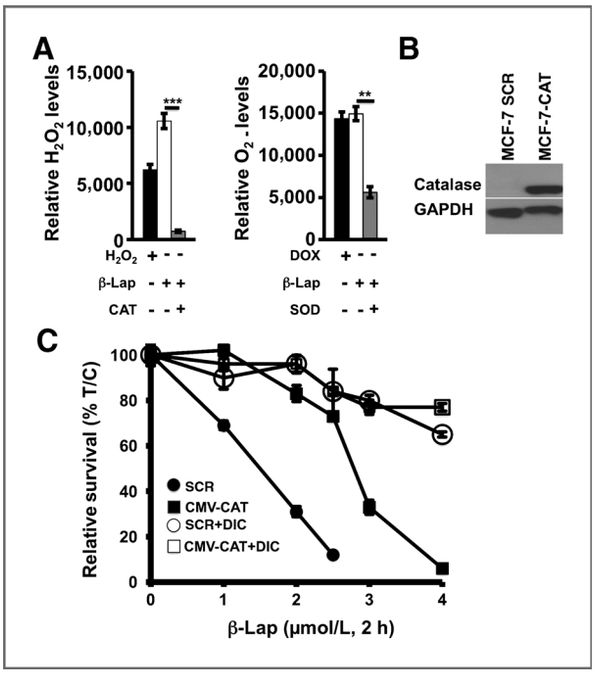

Figure 4. Catalase prevents β-lap–induced H_2O_2 formation and enhances clonogenic survival. A, 231-NQ+ cells were treated with β-lap (4 μmol/L) in the presence or absence of 1,000 U catalase or 3,000 U CuZnSOD and stained with DHE or DCFDA for superoxide or H_2O_2 formation, respectively, as in Fig. 1. H_2O_2 (200 μmol/L) or DOX (5 μmol/L) exposures were for 30 minutes as positive controls. Shown are means ± SE of integrated density values from representative digital images of at least 100 cells. Data are from experiments conducted 3 independent times in triplicate. **, $P \leq 0.01$; ***, $P \leq 0.001$. B, MCF-7 cells were transiently transfected with a CMV-driven catalase (CMV-CAT) expression vector or SCR, from Open Biosystems. Transfected MCF-7 cells were assayed for catalase expression by Western blot analysis. GAPDH levels were monitored as an internal loading control. C, MCF-7 cells were transiently transfected with CMV-CAT or SCR expression vectors. After 48 hours, cells were trypsinized, counted, and plated in 48-well dishes. After adhering for 24 hours, cells were treated with β-lap (closed circle or closed square represents SCR or CMV-CAT transfected MCF-7 cells, respectively) or β-lap+ dicoumarol (open circle or square represents SCR or CMV-CAT transfected MCF-7 cells, respectively) at the indicated doses and survival assessed.

(Fig. 5C); for example, only 125 U of catalase was required with CuZnSOD to reach the same protection as 500 U catalase alone (Fig. 5A and C, $P \leq 0.001$, respectively). CuZnSOD enhanced the cytoprotective effects of all catalase doses used (Fig. 5A and C, $P \leq 0.001$, respectively). Exogenous catalase did not influence the survival of β--lap-resistant 231-NQ− cells with or without CuZnSOD (Fig. 5D), because OCR and ROS formation did not occur in the absence of NQO1 (Fig. 1).

Catalase also significantly suppressed DNA damage in β-lap–exposed 231-NQ+ cells monitored by comet assays (Fig. 6A), whereas β-lap-resistant 231-NQ− cells formed no DNA lesions after β-lap treatment, with or without catalase (Fig. 6B). Consistently, catalase blocked β-lap–induced PARP1 hyperactivation (Fig. 6C, top), formation of γH2AX (Fig. 6C, bottom), NAD^+ loss (Fig. 6D), downstream programmed necrosis-induced

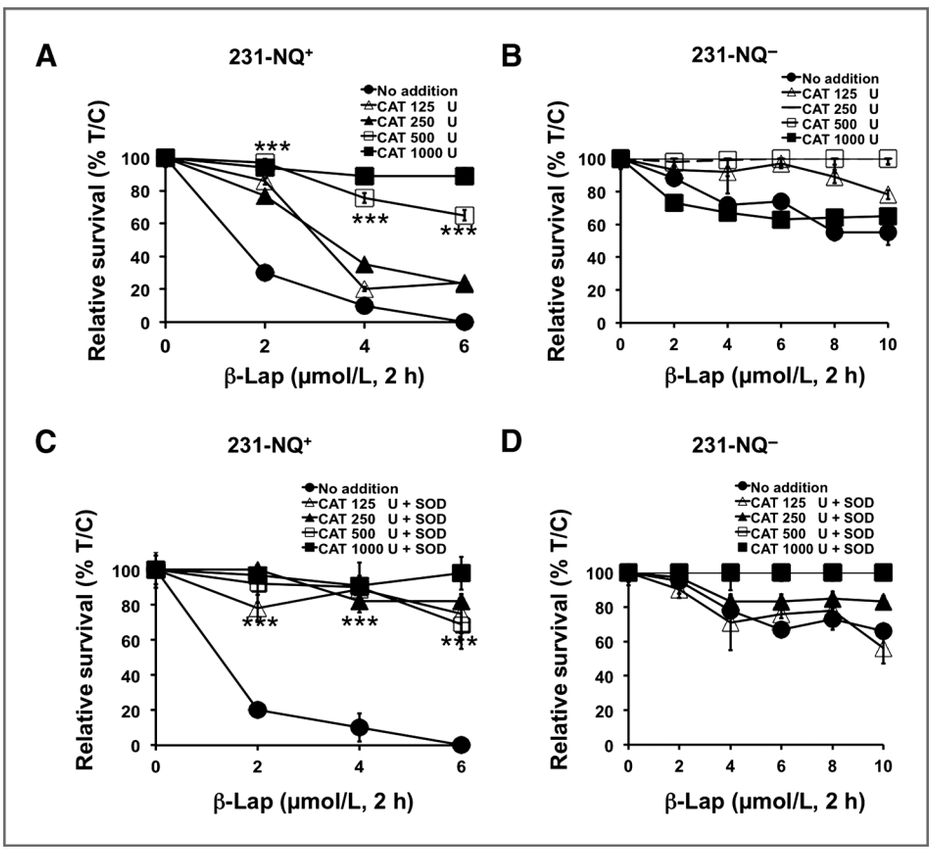

Figure 5. Exogenous catalase enhances clonogenic survival in MDA-MB 231-NQ+ cells. A and B, 231-NQ+ (A) or 231-NQ− (B) cells were treated with varying β-lap doses (μmol/L) with or without various catalase doses (U, units). Survival was assessed and results graphed as means ± SE of 3 experiments conducted in sextuplicate. C and D, 231-NQ+ or 231-NQ− cells were treated with various β-lap doses for 2 hours in the presence or absence of varying catalase doses, with or without 3,000 U CuZnSOD. Following 2-hour treatments, fresh media was added and survival assessed as in A and B. ***, $P \leq 0.001$.

atypical PARP1 and p53 proteolytic cleavage (Fig. 6E and Supplementary Fig. S5) and TUNEL+ responses (Fig. 6F) that are uniquely associated with NQO1 bioactivatable drug lethality.

β-Lap–induced programmed necrosis is accompanied by nuclear AIF translocation

β-Lap-treated MCF-7 cells (Supplementary Fig. S6) undergo atypical PARP1 and p53 proteolysis (15) due to μ-calpain activation (16, 25), whereas treatment of the same cells with staurosporine (STS) yielded classic apoptosis-related, ~89 kDa PARP1 proteolysis (Supplementary Fig. S6). BAPTA-AM, a calcium chelator, or DIC prevented β-lap–induced programmed necrosis. In contrast, the pan-caspase inhibitor, Z-VAD (see Supplementary Fig. S1 for structure), had no affect on β-lap–induced cell death or downstream PARP1/p53 proteolysis (Supplementary Fig. S6), but blocked STS-related PARP1 cleavage (26).

Because μ-calpain activation can stimulate downstream AIF translocation from mitochondria (9, 27), inducing programmed cell death (9), we examined a role for AIF in β-lap lethality. Indeed, activation and translocation of AIF from mitochondria (DMSO; Fig. 7A) to nuclei was noted (4–24 hours posttreatment; Fig. 7A) in β-lap–treated MCF-7 cells, consistent with μ-calpain activation kinetics (16, 25). AIF activation was blocked by BAPTA-AM (Fig. 7B) or catalase (1,000 U) cotreatments (Fig. 7C). However, siRNA-mediated AIF knockdown only partially decreased the lethal effects of β-lap in MCF-7 cells (Fig. 7D), most likely due to simultaneous activation of other cell death mediators, including posttranslational modification/activation of GAPDH (Fig. 8) that mediates apoptotic-like cell death (28). Stable AIF knockdown in MDA-MB-231 cells, like those recently reported (29), resulted in dramatic morphology and growth alterations, with similar partial blockage of lethality noted in β-lap–treated MCF-7 cells (Fig. 7D). Thus, β-lap stimulates multiple cell death factors, including μ-calpain (16, 25), AIF (Fig. 7), and S-nitrosylated GAPDH (Fig. 8).

Discussion

We used chemoresistant MDA-MB-231 TNBC cells to link NQO1-dependent futile cycling of β-lap to ROS-induced DNA damage and PARP1 hyperactivation. Threshold-level responses in cells after β-lap treatments were noted by sharp dose-dependent trigger events, mediated by robust H_2O_2 formation that, in turn, caused both DNA damage and $Ca^{2+}{}_{ER}$ release, ultimately leading to PARP1 hyperactivation (Supplementary Fig. S7). H_2O_2 production was the obligate ROS inducing cell death after β-lap, because catalase administration alone protected cells. PARP1 hyperactivation, both in dose–response and

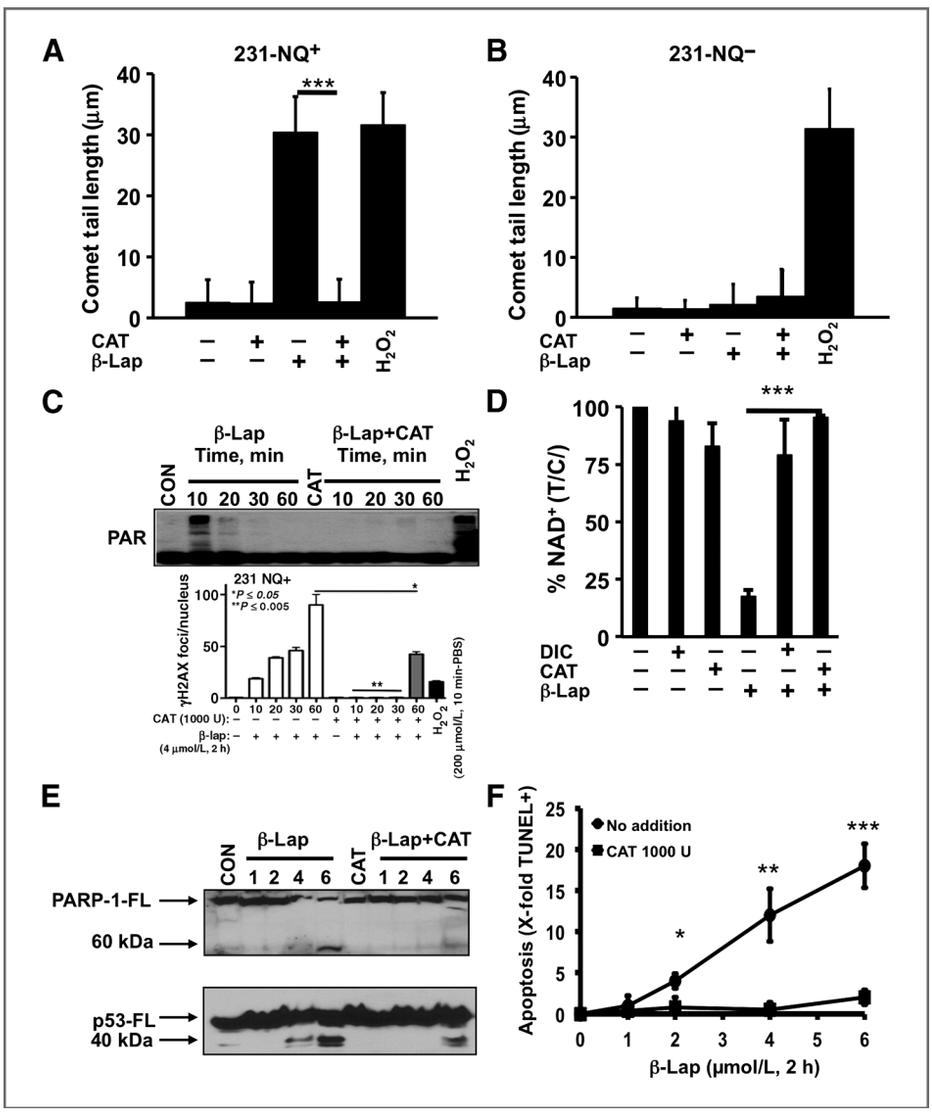

Figure 6. Exogenous catalase abrogates β-lap–induced cytotoxicity. A and B, 231-NQ+ or 231-NQ− cells were treated with β-lap (4 μmol/L, 2 hours) with or without catalase (1,000 U). Alkaline comet assays were then conducted (17). Shown are comet tail means ± SE of at least 50 comet tails per condition. Student *t* tests were conducted to determine significance between groups. ***, $P \leq 0.001$. C (top), 231-NQ+ cells were treated with 4 μmol/L β-lap as indicated with (right) or without (left) catalase (1,000 U). H_2O_2 (200 μmol/L, 60 minutes) was used a positive control. Whole-cell lysates were assessed for PARP1 hyperactivation (PAR-PARP1). γ-H2AX foci levels were assessed (bottom) in 231-NQ+ cells exposed to 4 μmol/L β-lap (with or without 1,000 U of catalase) or 200 μmol/L H_2O_2. Foci formed in individual cells were assessed microscopically as described previously (17). D, 231-NQ+ cells were treated with β-lap (4 μmol/L, 2 hours), with or without catalase (1,000 U), and with or without 40 μmol/L DIC. Cells were analyzed for NAD^+ levels as in Fig. 3 and data presented as means ± SE from 3 experiments conducted in triplicate each. ***, $P \leq 0.001$. E, 231-NQ+ cells were treated with varying doses of β-lap for 2 hours with (right) or without (left) catalase (1,000 U). Whole-cell lysates were analyzed for PARP1 and p53 proteolysis (15). F, 231-NQ+ cells were treated with various β-lap doses (1, 2, 4, or 6 μmol/L) with or without catalase (1,000 U) for 2 hours and populations analyzed for TUNEL+ staining 48 hours later (18). Data were graphed as X-fold TUNEL+ staining changes of β-lap–exposed versus DMSO-treated cells ±SE from 3 independent experiments repeated in triplicate. *, $P \leq 0.05$; **, $P \leq 0.01$; and ***, $P \leq 0.001$.

temporal kinetics of triggering cell death, resulted in catastrophic loss of essential nucleotides (NAD^+ and ATP) that correlated well with the "2 hours minimum time to death" induced by β-lap in NQO1+ expressing cells (17). Downstream, AIF activation and nuclear translocation (Fig. 7) were consistent with our prior findings of μ-calpain activation (25), and previously described role(s) of μ-calpain in AIF activation by others (30). However, AIF activation is one of a number of simultaneously activated cell death responses stimulated during β-lap–induced programmed necrosis, and we were not able to completely protect cells by AIF knockdown alone, as others suggested (29). Differences in AIF knockdown could explain the conflicting results, however, our identification of various cell death factors (e.g., μ-calpain, AIF, GAPDH modification, as well as loss of essential

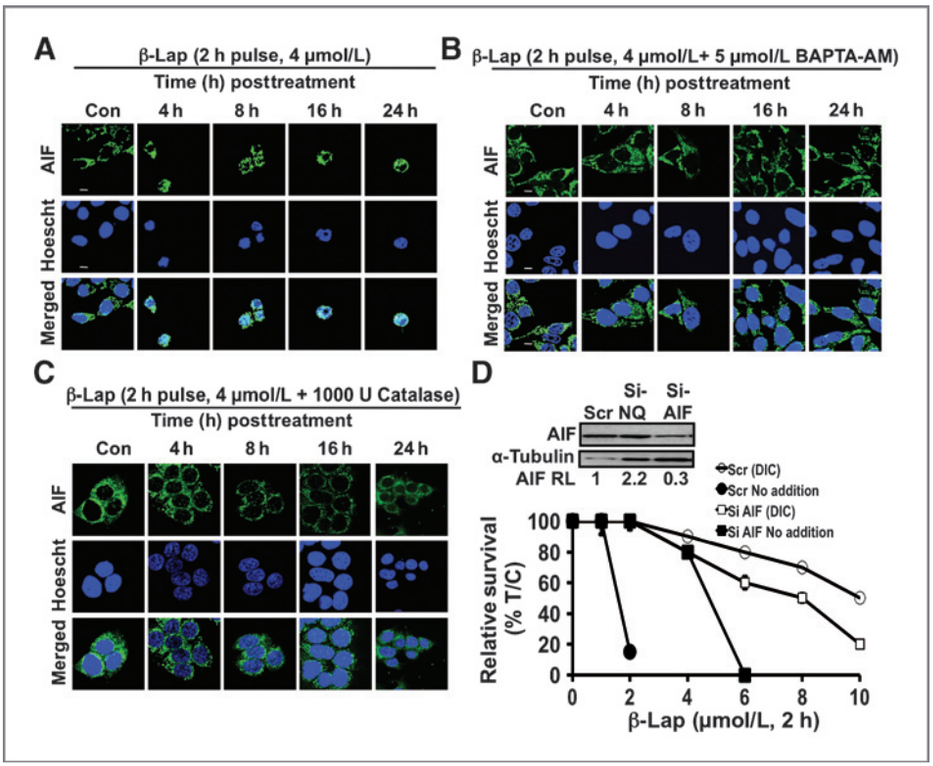

Figure 7. β-Lap–induced cell death factor activation is abrogated by exogenous catalase. A to C, MCF-7 cells were treated with β-lap (4 μmol/L, 2 hours) (A), ± BAPTA-AM (5 μmol/L) (B), or 1,000 U catalase (C). Cells were then fixed and stained for AIF expression and Hoescht as described (39) and representative confocal micrographs taken at 100× magnification. Both BAPTA-AM and catalase prevented AIF translocation from mitochondria to nuclei, and movement of mitochondria to perinuclear space. Mitochondria-specific staining confirmed AIF localization in organelles. D, MCF-7 cells were transiently transfected with 20 μmol/L siRNA specific for AIF or with scrambled nonsense siRNA as a control (40). Specific downregulation of AIF expression was confirmed by Western blotting (see inset) using α-tubulin as a loading control. AIF relative levels (RL) were assessed by comparing densitometry scans (NIH ImageJ software) of the loading control and AIF protein levels. Stable shRNA–AIF–transfected MCF-7 or MDA-MB-231 cells had altered growth rates and morphology and were not used. After 48 hours, cells were treated with various β-lap doses (μmol/L, 2 hours), with or without 40 μmol/L DIC and survival assessed as in Fig. 2.

nucleotides) simultaneously activated in β-lap–exposed NQO1+ cells, make it unlikely that AIF abrogation alone would spare most β-lap–exposed solid cancer cells. Although not explored in detail, the posttranslational modification of GAPDH in β-lap–treated NQO1+ cells has potentially important implications for understanding β-lap–induced cell "clean-up." S-nitrosylation of GAPDH implies a potentially important role of nitric oxide species (NOS; ref. 28) in β-lap–induced lethality. GAPDH modification inhibits its functions in glycolysis (31, 32) and activates its DNA repair (33) and cell death (34) functions, suggesting dramatic metabolic changes in exposed cancer cells due to this agent. Exposure to therapeutic β-lap doses caused supra-lethal ROS levels and DNA damage that was not repaired, presumably due to loss of NAD^+/ATP within ~60 minutes of exposure (Fig. 3B). We are currently exploring the roles of NOS and posttranslational GAPDH in altered metabolism and repair in NQO1+ cells exposed to β-lap.

We present the first evidence that H_2O_2 is the primary obligate ROS species necessary for β-lap's lethal effects. A primary role for H_2O_2 is also consistent with the specific induction of SSBs caused by this promising tumor-selective antitumor agent. CuZnSOD specifically enhanced the efficacy of catalase to block β-lap cytotoxicity in NQO1+ cancer cells. These data predict that normal tissue, which typically has higher catalase levels than cancer cells (35–37), could be selectively spared from toxicity caused by this agent. Alternatively, cancer cells overexpressing catalase and/or CuZnSOD would require higher doses of β-lap to avoid "sublethal therapeutic treatments." Accordingly, we propose that the ratio of NQO1 to catalase expression in tumor versus normal tissue is a major determinant of tumor selectivity for β-lap and future drugs that work by "NQO1 bioactivation." On this point, it is interesting that an inverse correlation between NQO1 expression and catalase is noted across breast cancer cells (Supplementary Fig. S8). We also noted that catalase expression in breast cancer cells was commonly low and did not dramatically affect the lethality of β-lap–treated breast cancer cells that overexpress NQO1. We predict that NQO1/catalase ratio calculations are important when examining normal tissue versus tumor tissue, but that β-lap–exposed NQO1 overexpressing cells will

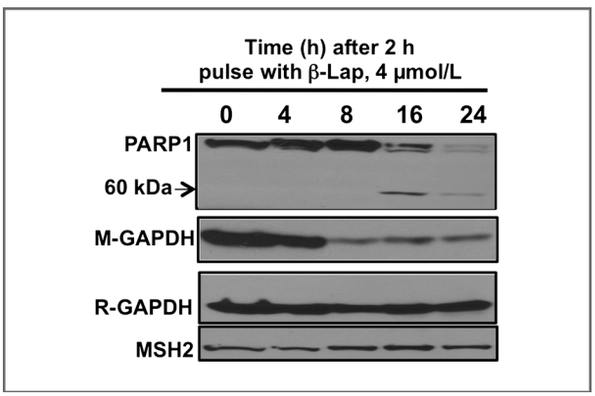

Figure 8. GAPDH proteolysis is induced during β-Lap–induced cell death. MCF-7 cells were treated with β-lap (4 μmol/L, 2 hours) and whole-cell extracts monitored for PAR-PARP1, S-nitrosylated GAPDH (M-GAPDH), or total GAPDH (R-GAPDH) using antibodies that detect a specific site known to be S-nitrosylated (41) or a polyclonal antibody to GAPDH, respectively. MSH2 levels were monitored as an internal loading control.

respond whether catalase is expressed or not, since ROS production can overwhelm catalase-mediated scavenging due to the futile cycle (Fig. 1A).

Catalase protects cells from H_2O_2-induced lipid peroxidation that damages membranes and cellular organelles. Although exogenous catalase enhanced survival at low doses, excessive ROS and NOS formation by higher β-lap doses (>6 μmol/L) were not inhibited by catalase alone. Although CuZnSOD alone did not spare β-lap–exposed NQO1+ cells, it enhanced the cytoprotective capacity of catalase. Combining CuZnSOD with catalase presumably converted superoxide to $2H_2O_2$ that was easily detoxified by catalase to $O_2 + 2H_2O$.

β-Lap-treated NQO1+ breast cancer cells, including TNBC cells, produce supra-lethal levels of ROS due to futile cycle metabolism of β-lap specifically by NQO1. The mechanism of action of this agent involves PARP1 hyperactivation that triggers simultaneous redundant downstream lethal events, including essential nucleotide loss (NAD^+ and ATP), AIF release, S-nitrosylation of GAPDH, and eventually programmed necrosis. Identification of ROS-scavenging enzymes (i.e., SOD, catalase) that can partially suppress β-lap–induced lethality is a crucial step in understanding resistance factors for this agent. Interrogation of expression of these factors may allow us to predict efficacious doses required for improved efficacy of NQO1 bioactivatable drugs, such as β-lap, DNQ, and their derivatives. Because NQO1 levels are overexpressed in breast cancer versus adjacent normal tissue (11), and particularly in ER+ breast cancer patients (38), these data strongly indicate use of this agent against breast, as well as many other solid tumors that specifically overexpressed NQO1. Monitoring NQO1/catalase ratios in tumor versus normal tissue will be essential for "personalized therapies" using β-lap or other NQO1 bioactivatable drugs.

Disclosure of Potential Conflicts of Interest

J. Gao is a consultant/advisory board member for StemPar Sciences, Inc.. D.A. Boothman is a consultant/advisory board member for StemPAR Sciences, Inc. No potential conflicts of interest were disclosed by the other authors.

Authors' Contributions

Conception and design: E.A. Bey, M.C. Srougi, L. Cao, Z. Moore, W.G. Bornmann, D.J. Buchsbaum, D.R. Spitz, J. Gao, D.A. Boothman

Development of methodology: E.A. Bey, M.C. Srougi, M. Varnes, V.E. Anderson, J.J. Pink, L. Cao, Z. Moore, W.G. Bornmann, D.R. Spitz, D.A. Boothman

Acquisition of data (provided animals, acquired and managed patients, provided facilities, etc.): E.A. Bey, K.E. Reinicke, V.E. Anderson, L. Cao, Z. Moore, A. Rommel, C. Lewis, D.M. Euhus, W.G. Bornmann, D.J. Buchsbaum, D.R. Spitz, D.A. Boothman

Analysis and interpretation of data (e.g., statistical analysis, biostatistics, computational analysis): E.A. Bey, K.E. Reinicke, M.C. Srougi, L.S. Li, M. Patel, L. Cao, Z. Moore, A. Rommel, D.J. Buchsbaum, D.R. Spitz, D.A. Boothman

Writing, review, and/or revision of the manuscript: E.A. Bey, K.E. Reinicke, L. Cao, Z. Moore, M. Boatman, D.J. Buchsbaum, D.R. Spitz, J. Gao, D.A. Boothman

Administrative, technical, or material support (i.e., reporting or organizing data, constructing databases): E.A. Bey, M. Varnes, L.S. Li, L. Cao, Z. Moore, M. Boatman, D.A. Boothman

Study supervision: E.A. Bey, V.E. Anderson, L. Cao, Z. Moore, D.A. Boothman

Acknowledgments

This article is dedicated to Dr. M. Varnes, Emeritus Professor of Radiation Oncology, CWRU, who began these studies. The authors also thank the imaging, mouse metabolism, and flow cytometry cores, Simmons Comprehensive Cancer Center.

Grant Support

This work was supported by NIH/NCI grant CA102792 to D.A. Boothman and DoD Breast Cancer Pre-Doctoral Fellowships to K.E. Reinicke (W81XWH-05-1-0248) and M.C. Srougi (W81XWH-04-1-0301). Grant CA13314 supported D.R. Spitz, as did CA086862, the Radiation and Free Radical Research Core. This work was also supported by a Susan G. Komen grant (KG090969) and NIH grant PS0 CA089019 to D.J. Buchsbaum.

The costs of publication of this article were defrayed in part by the payment of page charges. This article must therefore be hereby marked *advertisement* in accordance with 18 U.S.C. Section 1734 solely to indicate this fact.

Received October 3, 2012; revised June 24, 2013; accepted July 18, 2013; published OnlineFirst July 24, 2013.

References

1. Jemal A, Siegel R, Xu J, Ward E. Cancer statistics, 2010. CA Cancer J Clin 2010;60:277–300.
2. Pohlmann PR, Mayer IA, Mernaugh R. Resistance to trastuzumab in breast cancer. Clin Cancer Res 2009;15:7479–91.
3. Moreno-Aspitia A, Perez EA. Treatment options for breast cancer resistant to anthracycline and taxane. Mayo Clin Proc 2009;84:533–45.
4. May CD, Sphyris N, Evans KW, Werden SJ, Guo W, Mani SA. Epithelial-mesenchymal transition and cancer stem cells: a dangerously dynamic duo in breast cancer progression. Breast Cancer Res 2011;13:202.
5. O'Brien CS, Howell SJ, Farnie G, Clarke RB. Resistance to endocrine therapy: are breast cancer stem cells the culprits? J Mammary Gland Biol Neoplasia 2009;14:45–54.
6. Kaufmann SH, Vaux DL. Alterations in the apoptotic machinery and their potential role in anticancer drug resistance. Oncogene 2003;22:7414–30.

7. Huang X, Dong Y, Bey EA, Kilgore JA, Bair JS, Li LS, et al. An NQO1 substrate with potent antitumor activity that selectively kills by PARP1-induced programmed necrosis. Cancer Res 2012;72:3038–47.
8. Zong WX, Ditsworth D, Bauer DE, Wang ZQ, Thompson CB. Alkylating DNA damage stimulates a regulated form of necrotic cell death. Genes Dev 2004;18:1272–82.
9. Yu SW, Wang H, Poitras MF, Coombs C, Bowers WJ, Federoff HJ, et al. Mediation of poly(ADP-ribose) polymerase-1-dependent cell death by apoptosis-inducing factor. Science 2002;297:259–63.
10. Zong WX, Thompson CB. Necrotic death as a cell fate. Genes Dev 2006;20:1–15.
11. Marin A, Lopez de Cerain A, Hamilton E, Lewis AD, Martinez-Penuela JM, Idoate MA, et al. DT-diaphorase and cytochrome B5 reductase in human lung and breast tumours. Br J Cancer 1997;76:923–9.
12. Dong Y, Bey EA, Li LS, Kabbani W, Yan J, Xie XJ, et al. Prostate cancer radiosensitization through poly(ADP-Ribose) polymerase-1 hyperactivation. Cancer Res 2010;70:8088–96.
13. Lewis AM, Ough M, Hinkhouse MM, Tsao MS, Oberley LW, Cullen JJ. Targeting NAD(P)H:quinone oxidoreductase (NQO1) in pancreatic cancer. Mol Carcinog 2005;43:215–24.
14. Boothman DA, Trask DK, Pardee AB. Inhibition of potentially lethal DNA damage repair in human tumor cells by β-lapachone, an activator of topoisomerase I. Cancer Res 1989;49:605–12.
15. Pink JJ, Planchon SM, Tagliarino C, Varnes ME, Siegel D, Boothman DA. NAD(P)H:Quinone oxidoreductase activity is the principal determinant of β-lapachone cytotoxicity. J Biol Chem 2000;275:5416–24.
16. Tagliarino C, Pink JJ, Dubyak GR, Nieminen AL, Boothman DA. Calcium is a key signaling molecule in β-lapachone-mediated cell death. J Biol Chem 2001;276:19150–9.
17. Bentle MS, Reinicke KE, Bey EA, Spitz DR, Boothman DA. Calcium-dependent modulation of poly(ADP-ribose) polymerase-1 alters cellular metabolism and DNA repair. J Biol Chem 2006;281:33684–96.
18. Bey EA, Bentle MS, Reinicke KE, Dong Y, Yang CR, Girard L, et al. An NQO1- and PARP-1-mediated cell death pathway induced in non-small-cell lung cancer cells by β-lapachone. Proc Natl Acad Sci U S A 2007;104:11832–7.
19. Li LS, Bey EA, Dong Y, Meng J, Patra B, Yan J, et al. Modulating endogenous NQO1 levels identifies key regulatory mechanisms of action of β-lapachone for pancreatic cancer therapy. Clin Cancer Res 2011;17:275–85.
20. Bentle MS, Bey EA, Dong Y, Reinicke KE, Boothman DA. New tricks for old drugs: the anticarcinogenic potential of DNA repair inhibitors. J Mol Histol 2006;37:203–18.
21. Reinicke KE, Bey EA, Bentle MS, Pink JJ, Ingalls ST, Hoppel CL, et al. Development of β-lapachone prodrugs for therapy against human cancer cells with elevated NAD(P)H:quinone oxidoreductase 1 levels. Clin Cancer Res 2005;11:3055–64.
22. Zhao W, Spitz DR, Oberley LW, Robbins ME. Redox modulation of the pro-fibrogenic mediator plasminogen activator inhibitor-1 following ionizing radiation. Cancer Res 2001;61:5537–43.
23. Goshe MB, Anderson VE. Hydroxyl radical-induced hydrogen/deuterium exchange in amino acid carbon-hydrogen bonds. Radiat Res 1999;151:50–8.
24. Lowry OH, Rosebrough NJ, Farr AL, Randall RJ. Protein measurement with the Folin phenol reagent. J Biol Chem 1951;193:265–75.
25. Tagliarino C, Pink JJ, Reinicke KE, Simmers SM, Wuerzberger-Davis SM, Boothman DA. Mu-calpain activation in β-lapachone-mediated apoptosis. Cancer Biol Ther 2003;2:141–52.
26. Casiano CA, Ochs RL, Tan EM. Distinct cleavage products of nuclear proteins in apoptosis and necrosis revealed by autoantibody probes. Cell Death Differ 1998;5:183–90.
27. Hong SJ, Dawson TM, Dawson VL. Nuclear and mitochondrial conversations in cell death: PARP-1 and AIF signaling. Trends Pharmacol Sci 2004;25:259–64.
28. Hara MR, Agrawal N, Kim SF, Cascio MB, Fujimuro M, Ozeki Y, et al. S-nitrosylated GAPDH initiates apoptotic cell death by nuclear translocation following Siah1 binding. Nat Cell Biol 2005;7:665–74.
29. Lee H, Park MT, Choi BH, Oh ET, Song MJ, Lee J, et al. Endoplasmic reticulum stress-induced JNK activation is a critical event leading to mitochondria-mediated cell death caused by β-lapachone treatment. PLoS One 2011;6:e21533.
30. Polster BM, Basanez G, Etxebarria A, Hardwick JM, Nicholls DG. Calpain I induces cleavage and release of apoptosis-inducing factor from isolated mitochondria. J Biol Chem 2005;280:6447–54.
31. Colell A, Green DR, Ricci JE. Novel roles for GAPDH in cell death and carcinogenesis. Cell Death Differ 2009;16:1573–81.
32. Mohr S, Stamler JS, Brune B. Posttranslational modification of glyceraldehyde-3-phosphate dehydrogenase by S-nitrosylation and subsequent NADH attachment. J Biol Chem 1996;271:4209–14.
33. Sirover MA. Minireview. Emerging new functions of the glycolytic protein, glyceraldehyde-3-phosphate dehydrogenase, in mammalian cells. Life Sci 1996;58:2271–7.
34. Dastoor Z, Dreyer JL. Potential role of nuclear translocation of glyceraldehyde-3-phosphate dehydrogenase in apoptosis and oxidative stress. J Cell Sci 2001;114:1643–53.
35. Alexander NM. Catalase inhibition by normal and neoplastic tissue extracts. J Biol Chem 1957;227:975–85.
36. Bannister WH, Bannister JV. Factor analysis of the activities of superoxide dismutase, catalase and glutathione peroxidase in normal tissues and neoplastic cell lines. Free Radic Res Commun 1987;4:1–13.
37. Sihto H, Lundin J, Lundin M, Lehtimaki T, Ristimaki A, Holli K, et al. Breast cancer biological subtypes and protein expression predict for the preferential distant metastasis sites: a nationwide cohort study. Breast Cancer Res 2011;13:R87.
38. Jamshidi M, Bartkova J, Greco D, Tommiska J, Fagerholm R, Aittomaki K, et al. NQO1 expression correlates inversely with NFκB activation in human breast cancer. Breast Cancer Res Treat 2012;132:955–68.
39. Chiu SM, Oleinick NL. Dissociation of mitochondrial depolarization from cytochrome c release during apoptosis induced by photodynamic therapy. Br J Cancer 2001;84:1099–106.
40. Ough M, Lewis A, Bey EA, Gao J, Ritchie JM, Bornmann W, et al. Efficacy of β-lapachone in pancreatic cancer treatment: exploiting the novel, therapeutic target NQO1. Cancer Biol Ther 2005;4:95–102.
41. Schonhoff CM, Matsuoka M, Tummala H, Johnson MA, Estevez AG, Wu R, et al. S-nitrosothiol depletion in amyotrophic lateral sclerosis. Proc Natl Acad Sci U S A 2006;103:2404–9.